

Two orthotropic models for strain-induced anisotropy of polar ice

R. STAROSZCZYK,¹ O. GAGLIARDINI²

¹*School of Mathematics, University of East Anglia, Norwich NR4 7TJ, England*

²*Laboratoire de Glaciologie et Géophysique de l'Environnement du C.N.R.S, BP96, 38402 Saint-Martin-d'Hères Cedex, France*

ABSTRACT. As polar ice descends from the free surface to depth in a large ice sheet, it undergoes deformations which give rise to the formation and subsequent evolution of a fabric and associated anisotropy. In this paper two orthotropic models of such strain-induced anisotropy are considered. Model A is based on analysis of the microscopic behaviour of an individual ice crystal with transversely isotropic response and assumed uniform stress in a polycrystal. The macroscopic response of the ice aggregate is then derived by applying the concept of an orientation distribution function, and the resulting viscous law relates the strain rate to the stress and three structure tensors. In model B it is assumed that the macroscopic response of ice is determined by the fabric induced entirely by macroscopic deformations, and all microprocesses taking place at the grain level are ignored. A constitutive relation is derived from a general frame-indifferent law for orthotropic materials, and expresses the stress in terms of the strain rate, strain and three structure tensors. The two models are applied to determine the viscous response of ice to continued uniaxial compression and simple shearing in order to compare the predictions of both theories.

1. INTRODUCTION

Polar ice cores drilled at different sites in Antarctica and Greenland (Gow and Williamson, 1976; Russell-Head and Budd, 1979; Herron and Langway, 1982; Lipenkov and others, 1989) reveal strong fabrics, with significant alignment of c axes of individual crystals along some preferential directions, induced by strains to which the ice is subject as it descends from the free surface to depth in an ice sheet. The fabric created during the ice deformation gives rise to macroscopic anisotropy of the medium which considerably affects polar ice-sheet dynamic behaviour over long time-scales. This has been confirmed by numerical simulations carried out by Mangeney and others (1996), who have applied a transversely isotropic flow law, with a rotational symmetry axis assumed to be vertical everywhere, to the ice-sheet flow problem with a non-evolving ice fabric derived from the measurements made along the GRIP ice core (Thorsteinsson and others, 1997). It has been found that for a given, fixed in time, free-surface elevation the assumption of the ice anisotropy results in much faster ice flow compared to the isotropic case, and an estimated accumulation rate required to maintain a steady-state flow exceeds by more than 1.5 times the rate for isotropic ice. Similar conclusions have been drawn by Mangeney and others (1997), who considered a more realistic problem in which the free-surface elevation was calculated for a fixed accumulation rate. Their numerical results showed that the ice anisotropy, as well as leading to a globally faster flow, significantly increases shear stresses near the bedrock, makes the free surface flatter in the ice-divide region, and smooths out the effects of the bed topography. This clearly indicates that the strain-induced anisotropy must be included in any large-scale numerical model of polar ice sheets if realistic results are to be obtained. How-

ever, there is still no generally accepted constitutive law describing the anisotropic behaviour of polar ice. This is partly because of the complexity of physical phenomena taking place on the microscale of single crystals during the fabric formation, but also because of difficulties associated with the mathematical modelling of the strain-induced, evolving in time, anisotropy.

Following Lliboutry and Duval (1985) and Alley (1992), we distinguish three main regions along the depth of a typical polar ice sheet in accordance with the microscopic processes which dominate the ice-fabric evolution.

- (1) In the upper part of a large ice sheet, extending from approximately 100 m under the free surface to about one-third of its thickness, shear stresses are negligibly small compared to normal stresses. Deformation is mainly due to dislocation glide on basal planes, and c axes of grains rotate towards compressional axes. The grain-size increases linearly with the age of ice, which is here nearly proportional to its depth, and no new grains are created.
- (2) Between approximately one-third and two-thirds of the ice cap thickness, the shear stresses gradually increase, though they are still smaller than the normal stresses. With increasing deformation and strain energy stored in grains, the fabric continues to strengthen and the process of *polygonisation* (also called *rotation recrystallisation*) occurs. In this process new grains, with orientations similar to old grains which are not consumed by new nuclei, are produced. The average grain-size changes little with depth throughout this region.
- (3) In the region directly over the bedrock, the shear stresses dominate the normal stresses, which combined with high temperatures initiates the process of *migration* (or

dynamic) recrystallisation. New, strain-free, grains with their c axes at high angles ($\sim 45^\circ$) to compressional axes are created at the expense of old grains which are consumed by new nuclei. Abrupt changes in the average grain-size are usually observed in this region, but generally the grains are much larger than in region 2.

In order to construct a macroscopic constitutive law for anisotropic polycrystalline ice, a basic and physically motivated approach is to derive an average response of ice aggregate from the properties of individual grains and assumptions on crystal interactions. To date, most of the existing anisotropic models include only the mechanism of the grain c -axis rotation, which dominates the fabric formation and evolution in the upper part of an ice sheet, although some attempts to incorporate the recrystallisation process, prevailing in deeper regions of ice sheets, have already been made. Azuma (1994) and Azuma and Goto-Azuma (1996) assume that individual crystals deform only by basal glide, the glide direction is determined by that of the maximum macroscopic shear stress in the polycrystal, and the crystal (microscopic) and polycrystal (macroscopic) stresses, which may be different in this model, are related by a geometric tensor associated with the c -axis and glide directions. Lliboutry (1993) assumes that the microscopic stress acting on each individual grain is equal to the bulk macroscopic stress applied to the polycrystal, and formulates a flow law for a transversely isotropic aggregate. Castelnau and Duval (1994) and Van der Veen and Whillans (1994) extended Lliboutry's homogeneous stress model (also called the static model) to any type of evolving anisotropy by considering a polycrystal consisting of a finite number of grains. Van der Veen and Whillans (1994) are the first to include the recrystallisation mechanism in their model, and consider two alternative criteria to determine the onset of recrystallisation in terms of threshold accumulated strains of crystals. Another, more general, approach is the visco-plastic self-consistent (VPSC) model developed by Castelnau and others (1996). In this formulation, the single crystal is treated as an embedded idealised geometric inclusion in an infinite medium with properties of an assumed form supposed to represent the macroscopic behaviour. In contrast to the models discussed above, in which individual crystals can glide only on basal planes, in the VPSC model crystal slips on basal, prismatic and pyramidal planes are considered, and stresses and strain rates are assumed to depend on the crystallographic orientation.

In all the above theories, which can be called discrete grain models, usually about 200–400 grains are needed to properly describe the ice fabric at a given point. Since in typical large-scale numerical models for ice-sheet flows the number of mesh nodes can exceed 10^5 , it is obvious that discrete grain models are not suitable for simulations run on currently available computers. Therefore, in order to significantly reduce the number of variables involved in the description of ice fabric, another approach, in which the polycrystalline aggregate is treated as a continuum, has been adopted. In this approach a so-called orientation distribution function (ODF), defining continuous weightings to the grain c -axis orientation, has been applied. Although the concept of the ODF is already well established in material science (Bunge, 1982), it was first introduced to the field of theoretical glaciology only recently by Lliboutry (1993), Meyssonier and Philip (1996) and Svendsen and Hutter (1996). Meyssonier and

Philip (1996) formulated a transversely isotropic flow law for a polycrystalline ice using the ODF concept and the VPSC model by adopting some simplifying assumptions on the single grain behaviour, namely, that the crystal is transversely isotropic and offers small resistance to shearing parallel to its basal planes, and the response is governed by a linearly viscous law. Svendsen and Hutter (1996) employed the ODF approach to derive analytically a frame-indifferent viscous law which incorporates the fabric through a single structure tensor defined by an axis of assumed transverse isotropy. This theory has been considerably extended by Gödert and Hutter (1998, in press). However, the complicated calculations required to follow the evolving properties of individual ice elements will add considerably to numerical treatments of large ice-sheet flows. A transversely isotropic flow law that avoids the use of an orientation distribution function has been proposed by Van der Veen and Whillans (1990). They modify Johnson's (1977) law for a transversely isotropic viscoelastic solid by replacing material measures of stress and strain rate by spatial measures. However, they include the vertical (gravity) direction in the material structure, so this model cannot be treated as a valid constitutive relation for the response to general loading.

Dependence of the fabric on ice deformation implies that transverse isotropy of the medium can occur only if the flow in the ice sheet induces uniform stretches in some plane, say a horizontal plane in a gravity-dominated flow under a central dome, in which case a transversely isotropic fabric with the vertical as its rotational symmetry axis develops. Elsewhere in the ice sheet, however, such particular symmetry of the ice flow does not take place in general, and consequently the ice deformation, and hence the ice fabric, does not have rotational symmetry about any axis. Therefore, in order to more realistically describe the strain-induced ice fabric, a more general form of anisotropy is needed. Such increased generality is offered by orthotropic models. Although, strictly, the orthotropy does not occur for any arbitrary loading because of the fabric evolution which destroys any (already developed) orthotropic symmetries in the material, the assumption of orthotropy is strongly supported by observational data showing that the fabric in ice sheets does, in fact, usually reveal this type of material symmetry (this is in part due to the dynamic recrystallisation, not considered here, which helps to sustain the earlier created orthotropy despite the changes in the strain configuration).

In the paper, two orthotropic viscous models are presented. The first model, formulated by Gagliardini and Meyssonier (in press), stems from analysis of the behaviour of a single ice grain in a polycrystal under the assumption of stress homogeneity, following Lliboutry (1993) and Van der Veen and Whillans (1994). Assuming transverse isotropy for each individual crystal and a linear response to deviatoric stresses, the macroscopic strain rate of the aggregate is derived by applying the ODF concept. Compared to Meyssonier and Philip (1996), Svendsen and Hutter (1996) and Gödert and Hutter (1998), additional parameters are introduced into the ODF. Owing to the extra parameters, the derivation of a macroscopically orthotropic (instead of transversely isotropic) viscous law relating the strain rate to the deviatoric stress and three structure tensors is possible.

The second orthotropic model considered here has been formulated by Morland and Staroszczyk (1998) and further extended by Staroszczyk and Morland (in press). In this approach it is assumed that the macroscopic mechanical re-

sponse of ice can be described in terms of the fabric induced purely by macroscopic deformation, and all microscopic processes occurring at the grain level are ignored. The assumption that the induced anisotropy depends only on the current strains and not on the deformation history is a considerable simplification since, in general, the fabric evolution is a path-dependent process. It is believed, however, that this approximation is the simplest approach to an evolving anisotropic viscous law that could be tractable in large-scale sheet dynamics, since it requires that only current deformation gradients are calculated in addition to the velocity and pressure fields. The constitutive relation is derived from the general frame-indifferent orthotropic representation (Boehler, 1987), and expresses the deviatoric stress in terms of the current strain rate, deformation and three structure tensors. The relation is separable in the isotropic dependence on strain rate and fabric dependence on deformation, and in its simplified form has only one independent fabric function that fully describes the orthotropic viscous response of ice. Although in this approach local interactions between individual crystals are excluded from the analysis, this method allows good qualitative agreement with observations, and flexibility to correlate with detailed experimental results.

The two orthotropic models are used to determine the viscous response of ice to simple stress and strain configurations, corresponding to those occurring in the uniaxial compression and simple shear tests carried out in a laboratory. The predictions of both theories are compared, and the influence of some model parameters on calculated responses is investigated. Additionally, the results for simple shear given by the micro-macroscopic model are compared with the results obtained from a discrete grain model (in which no assumptions are made about material symmetries) in order to verify the validity of the assumed orthotropic behaviour of polycrystalline ice.

2. MICRO-MACROSCOPIC MODEL

This model, formulated by Gagliardini and Meyssonier (in press), incorporates the basic micromechanism taking place on the grain level during the ice deformation, namely, the rotation of crystal c axes towards the axes of compression and away from the axes of extension. The macroscopic viscous-flow law which expresses the strain rates in terms of the deviatoric stresses is derived from the behaviour of individual grains by applying the homogenisation method based on the ODF approach.

In the following, three Cartesian reference frames are used to describe the behaviour of ice on the microscale of a single grain and the macroscale of a polycrystal:

- $\{R\}$ with axes x_i is a fixed global reference frame;
- $\{R^o\}$ is a privileged frame of an orthotropic polycrystal, whose axes x_i^o coincide with the orthogonal privileged directions in the material;
- $\{R^g\}$ with axes x_i^g is a local frame associated with an individual grain, whose x_3^g axis coincides with the c axis of this grain.

Microscopic quantities associated with an individual grain are indicated by a tilde, and superscripts "g" and "o" are used to denote non-scalar quantities expressed, respectively, in the local $\{R^g\}$ and the privileged orthotropic $\{R^o\}$ frames. Where no superscript is applied, respective symbols refer to

macroscopic quantities expressed in the global coordinate system $\{R\}$. Since the individual ice grain is assumed here to be transversely isotropic, with its c axis being the rotational symmetry axis, the grain position relative to the global reference frame $\{R\}$ can be uniquely described by means of two angles: the co-latitude (or zenith angle) θ and the longitude φ (see Fig. 1). These two angles determine the rotation matrix \mathbf{R} (cf. Meyssonier and Philip, 1996) which connects components of vectors and tensors in $\{R\}$ and $\{R^g\}$.

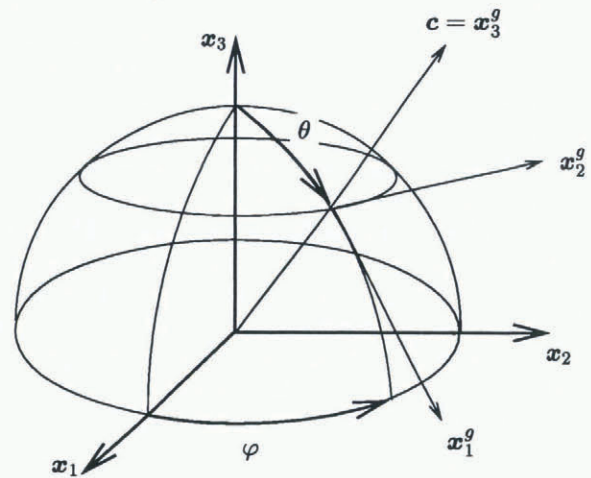


Fig. 1. Global and local reference frames, with angles θ and φ defining the c -axis orientation of a grain.

Following Llibouty (1993) and Van der Veen and Whilans (1994), the hypothesis of the stress homogeneity in ice aggregate has been adopted

$$\tilde{\sigma} = \sigma, \tag{1}$$

stating that the microscopic stress $\tilde{\sigma}$ in each grain, irrespective of the grain orientation, is equal to the macroscopic (bulk) stress σ applied to the polycrystal. The deviatoric stress σ' is defined by

$$\sigma' = \sigma + p\mathbf{I}, \quad p = -\frac{1}{3}\text{tr} \sigma, \quad \text{tr} \sigma' = 0, \tag{2}$$

where p is the mean pressure, \mathbf{I} is the unit tensor, and $\text{tr} \sigma$ denotes the trace of σ . Since the ice is assumed incompressible, p is a workless constraint not given by a constitutive law, but determined by the momentum balance and boundary conditions.

Further, it is assumed that the transversely isotropic crystal deforms mainly by simple shear parallel to its basal plane, and its response to stress is linearly viscous. Adopting the simple relation (Meyssonier and Philip, 1996) between the microscopic strain rate $\tilde{\mathbf{D}}$ and the microscopic deviatoric stress $\tilde{\sigma}'$, which is equal to the macroscopic stress σ' in view of Equation (1), the transversely isotropic flow law can be expressed in the form

$$\tilde{\mathbf{D}} = \frac{\psi}{2} \{ \beta \sigma' + (1 - \beta) [\sigma' \tilde{\mathbf{M}} + \tilde{\mathbf{M}} \sigma' - 2\text{tr}(\tilde{\mathbf{M}} \sigma') \tilde{\mathbf{M}}] \}, \tag{3}$$

where $\tilde{\mathbf{M}} = \mathbf{c} \otimes \mathbf{c}$ is the structure tensor defined in the global reference frame $\{R\}$ by the unit vector $\mathbf{c} = (\sin \theta \cos \varphi, \sin \theta \sin \varphi, \cos \theta)$ associated with the grain c axis, and ψ is the fluidity (reciprocal viscosity) for shearing parallel to the crystal basal plane. The parameter β is the ratio of the shear viscosity in a plane parallel to the c axis to the shear viscosity in a plane of isotropy (normal to the c axis) and can

be regarded as a measure of the grain anisotropy. When $\beta = 0$, the grain can deform only by basal glide, as assumed in the Lliboutry (1993) and Van der Veen and Whillans (1994) models, while $\beta = 1$ means that the grain is isotropic. In what follows it is also assumed that each grain in a polycrystal occupies the same volume and the number of grains does not change during the deformation, i.e. the grain growth, polygonisation and dynamic recrystallisation phenomena are not accounted for in this model.

The macroscopic (bulk) strain rate \mathbf{D} of the polycrystal, in response to the macroscopic deviatoric stress σ' , is defined as the average of the strain rates of its constituent grains. Various homogenisation techniques can be employed to calculate the average strain rates in the ice aggregate. In the discrete grain models (Azuma, 1994; Van der Veen and Whillans, 1994; Castelnau and others, 1996) with a finite number of grains, the components of \mathbf{D} are simply arithmetic means of the corresponding components of $\tilde{\mathbf{D}}$. In our continuum model with an infinite number of grains, we make use of the ODF concept, which describes the ice fabric in terms of the relative density of grains whose c axes have the orientation (θ, φ) in the global reference frame $\{R\}$. In the ODF approach, the weighted average of a quantity $\tilde{A}(\theta, \varphi)$ is defined by

$$A = \langle \tilde{A} \rangle = \frac{1}{2\pi} \int_0^{2\pi} \int_0^{\pi/2} \tilde{A}(\theta, \varphi) f(\theta, \varphi) \sin \theta \, d\theta \, d\varphi, \quad (4)$$

where $f(\theta, \varphi)$ is the proportion of grains with orientation (θ, φ) in the element "area" $\sin \theta \, d\theta \, d\varphi$, and by definition

$$\frac{1}{2\pi} \int_0^{2\pi} \int_0^{\pi/2} f(\theta, \varphi) \sin \theta \, d\theta \, d\varphi = 1. \quad (5)$$

Note that in the case of isotropy we have $f(\theta, \varphi) = 1$, and for transverse isotropy, with x_3 being the rotational symmetry axis, the ODF does not depend on φ , i.e. $f(\theta, \varphi) = f(\theta)$.

Hence, by the weighted average definition (Equation (4)), the components of the macroscopic strain rates in the global reference frame $\{R\}$ are given by

$$D_{ij} = \langle \tilde{D}_{ij} \rangle. \quad (6)$$

Once the ODF has been determined, Equations (3) and (6) yield the relation between the macroscopic strain rate \mathbf{D} and the deviatoric stress σ' . In order to describe the evolution of the ODF, consider the motion of the single grain, i.e. the rotation of its c axis in the global coordinate system $\{R\}$. Following Meyssonier and Philip (1996), the rotation matrix \mathbf{R} that defines the orientation of the grain in $\{R\}$ is governed by the relation

$$(\mathbf{R}^T \dot{\mathbf{R}} + \tilde{\mathbf{W}}^g - \mathbf{R}^T \tilde{\mathbf{W}} \mathbf{R}) \mathbf{c}^g = \mathbf{0}, \quad (7)$$

where \mathbf{R}^T is the transpose of \mathbf{R} , the superposed dot denotes the time derivative, $\tilde{\mathbf{W}}^g$ and $\tilde{\mathbf{W}}$ are spins (rates of rotation) of the grain in the local and global reference frames, respectively, and $\mathbf{c}^g = (0, 0, 1)$. Since during the grain deformation the original parallel glide planes remain parallel to each other, the velocity component along the crystal c axis, when expressed in the rotating frame $\{R^g\}$ attached to the grain, is a function of x_3^g only. This leads to the kinematic relations

$$\tilde{W}_{13}^g = \tilde{D}_{13}^g, \quad \tilde{W}_{23}^g = \tilde{D}_{23}^g, \quad (8)$$

which are a direct consequence of the adopted system of reference frames. In order to close the system of governing equations, three additional conditions are required, and

these are adopted by assuming that the microscopic and macroscopic spins are equal, i.e.

$$\tilde{\mathbf{W}} = \mathbf{W}. \quad (9)$$

The above equation is closely related to the Taylor (1938) assumption which postulates the equality of micro- and macroscopic velocity gradients. The combination of constraints (Equations (1) and (9)) adopted here is exactly the same as that used by Gödert and Hutter (1998). With Equations (8) and (9), Equation (7) provides two relations which describe the change in the grain orientation by

$$\dot{\theta} = -\tilde{D}_{13}^g + W_{13} \cos \varphi + W_{23} \sin \varphi, \quad (10)$$

$$\dot{\varphi} \sin \theta = -\tilde{D}_{23}^g - W_{12} \sin \theta + (W_{23} \cos \varphi - W_{13} \sin \varphi) \cos \theta. \quad (11)$$

Since recrystallisation is not taken into consideration, and hence the total number of grains in the polycrystal is conserved, it follows from the continuity equation (5) that the ODF satisfies the relation

$$\frac{\partial(f \sin \theta)}{\partial t} + \frac{\partial(\dot{\theta} f \sin \theta)}{\partial \theta} + \frac{\partial(\dot{\varphi} f \sin \theta)}{\partial \varphi} = 0. \quad (12)$$

Equations (10–12) completely describe the evolution of ice fabric for any type of macroscopic anisotropy that is based on the assumed behaviour of ice on the microscale of individual crystals. In the case of orthotropic anisotropy, the medium possesses three planes of reflexional symmetry, which in the reference frame $\{R^o\}$ are the planes (x_1^o, x_2^o) , (x_1^o, x_3^o) and (x_2^o, x_3^o) , and these material symmetries must be accounted for in the ODF. Following Meyssonier and Philip (1996), and using analytical results obtained by Gagliardini and Meyssonier (in press), we adopt the following form of the ODF:

$$f(\theta, \varphi, k_1, k_2, k_3, \varphi^o) = \left\{ \sin^2 \theta \left[k_1^2 \cos^2(\varphi - \varphi^o) + k_2^2 \sin^2(\varphi - \varphi^o) \right] + k_3^2 \cos^2 \theta \right\}^{-\frac{3}{2}}, \quad (13)$$

where k_1, k_2, k_3 and φ^o are parameters, the latter being the angle of rotation of the orthotropic frame $\{R^o\}$ with respect to the global reference frame $\{R\}$. Since the grain-conservation relation (Equation (5)) implies that $k_1 k_2 k_3 = 1$, only three parameters in Equation (13) are independent. Now, by substituting Equation (3) into Equation (6), and using Equation (13) in Equation (4), we obtain the orthotropic, linearly viscous law relating the macroscopic strain-rates to the macroscopic deviatoric stresses by

$$\mathbf{D} = \sum_{r=1}^3 \left[\alpha_r J_r \left(\mathbf{M}_r^o - \frac{1}{3} \mathbf{I} \right) + \alpha_{r+3} \left(\sigma' \mathbf{M}_r^o + \mathbf{M}_r^o \sigma' - \frac{2}{3} J_r \mathbf{I} \right) \right], \quad (14)$$

where $\mathbf{M}_r^o = \mathbf{e}_r^o \otimes \mathbf{e}_r^o$ are three structure tensors defined by the orthotropic axes unit vectors \mathbf{e}_r^o , and $J_r = \text{tr}(\mathbf{M}_r^o \sigma')$ are three invariants. The six response coefficients α_i

($i = 1, \dots, 6$) are functions of the grain rheological parameters ψ and β ,

$$\begin{bmatrix} \alpha_1 \\ \alpha_2 \\ \alpha_3 \\ \alpha_4 \\ \alpha_5 \\ \alpha_6 \end{bmatrix} = \frac{\psi(\beta - 1)}{2} \begin{bmatrix} 0 & -6 & 12 & 8 & -22 & 8 \\ 0 & 6 & -12 & -6 & 6 & 8 \\ 2 & -10 & 0 & 8 & 6 & -6 \\ \beta/[2(\beta-1)] & 1 & -3 & -2 & 6 & -2 \\ \beta/[2(\beta-1)] & -2 & 3 & 2 & -2 & -2 \\ (2-\beta)/[2(\beta-1)] & 3 & 0 & -2 & -2 & 2 \end{bmatrix} \begin{bmatrix} 1 \\ N_{30} \\ N_{32} \\ N_{50} \\ N_{52} \\ N_{54} \end{bmatrix}, \tag{15}$$

and $N_{30}, N_{32}, N_{50}, N_{52}, N_{54}$ are five moments defined by

$$N_{pq} = \frac{2}{\pi} \int_0^{\pi/2} \int_0^{\pi/2} f(\theta, \varphi) \sin^p \theta \sin^q \varphi \, d\theta \, d\varphi. \tag{16}$$

In the case of ice isotropy, i.e. when $f(\theta, \varphi) = 1$ and $k_1 = k_2 = k_3 = 1$, the above moments are

$$N_{30} = 2/3, N_{32} = 1/3, N_{50} = 8/15, N_{52} = 4/15, N_{54} = 1/5, \tag{17}$$

and the six material coefficients defined by Equation (15) become

$$\alpha_1 = \alpha_2 = \alpha_3 = 0, \quad \alpha_4 = \alpha_5 = \alpha_6 = \frac{\psi}{20}(3\beta + 2). \tag{18}$$

With the above parameters, and in view of the identity $\mathbf{M}_1^0 + \mathbf{M}_2^0 + \mathbf{M}_3^0 = \mathbf{I}$, the orthotropic constitutive law (Equation (14)) reduces to the linear Glen’s flow law for isotropic ice

$$\mathbf{D} = \frac{\psi_0}{2} \sigma', \tag{19}$$

where ψ_0 is the fluidity of the macroscopically isotropic polycrystal, which is related to the individual crystal fluidity ψ by

$$\psi_0 = \frac{\psi}{5}(3\beta + 2). \tag{20}$$

It follows from the latter formula that in the case of isotropic crystals ($\beta = 1$) the macroscopic fluidity ψ_0 equals the grain fluidity ψ while in the case of the most anisotropic crystals ($\beta = 0$), when the grain deformation occurs only by basal glide, $\psi_0 = 0.4\psi$.

3. CONTINUUM MODEL

In this continuum approach, proposed by Morland and Staroszczyk (1998) and further developed by Staroszczyk and Morland (in press), the phenomena taking place on the microscale of individual grains, as opposed to the model considered in section 2, are ignored, and it is assumed that the macroscopic response of ice depends only on the fabric induced solely by the macroscopic deformations. Although this is a considerable simplification, it is believed that such an approach to an evolving anisotropic constitutive law is well suited to the large-scale ice-sheet modelling, since it requires only that the deformation gradient field has to be determined during the ice flow in order to describe the fabric development. The chosen form of the orthotropic viscous law is the relation between the frame-indifferent deviatoric Cauchy stress σ' , current strain rate \mathbf{D} , Cauchy–Green strain tensor \mathbf{B} , and three structure tensors \mathbf{M}_r ($r = 1, 2, 3$) defined by the outer products of the current principal stretch axes unit vectors \mathbf{e}_r ($r = 1, 2, 3$).

Let Ox_i ($i = 1, 2, 3$) be spatial rectangular Cartesian coordinates with OX_i ($i = 1, 2, 3$) particle reference coordinates, and v_i the velocity components, then the deformation gradient \mathbf{F} and strain rate \mathbf{D} have the components

$$F_{ij} = \frac{\partial x_i}{\partial X_j}, \quad D_{ij} = \frac{1}{2} \left(\frac{\partial v_i}{\partial x_j} + \frac{\partial v_j}{\partial x_i} \right). \tag{21}$$

The strain \mathbf{B} , unit vectors \mathbf{e}_r ($r = 1, 2, 3$) and squares of the principal stretches b_r ($r = 1, 2, 3$) are defined by

$$\mathbf{B} = \mathbf{F}\mathbf{F}^T, \quad \mathbf{B}\mathbf{e}_r = b_r \mathbf{e}_r, \quad \det(\mathbf{B} - b_r \mathbf{I}) = 0, \quad b_r = \lambda_r^2 > 0, \tag{22}$$

where λ_r ($r = 1, 2, 3$) are principal stretches along the principal axes \mathbf{e}_r , and the three structure tensors \mathbf{M}_r are given by

$$\mathbf{M}_r = \mathbf{e}_r \otimes \mathbf{e}_r \quad (r = 1, 2, 3). \tag{23}$$

Ice is assumed incompressible, so

$$\det \mathbf{F} = \lambda_1 \lambda_2 \lambda_3 = \det \mathbf{B} = b_1 b_2 b_3 = 1, \quad \text{div } \mathbf{v} = 0. \tag{24}$$

In order to derive the macroscopic flow law for anisotropic ice, we follow Boehler’s (1987) theory for frame-indifferent relations between tensors and vectors, which ensures that material properties are independent of the observer. In the case of a symmetric tensor (here σ') being a function of two other symmetric tensors (here \mathbf{D} and \mathbf{B}), the general orthotropic representation is

$$\begin{aligned} \sigma' = \sum_{r=1}^3 & [\phi_r \mathbf{M}_r + \phi_{r+3}(\mathbf{M}_r \mathbf{D} + \mathbf{D} \mathbf{M}_r) \\ & + \phi_{r+6}(\mathbf{M}_r \mathbf{B} + \mathbf{B} \mathbf{M}_r)] \\ & + \phi_{10} \mathbf{D}^2 + \phi_{11} \mathbf{B}^2 + \phi_{12}(\mathbf{D} \mathbf{B} + \mathbf{B} \mathbf{D}), \end{aligned} \tag{25}$$

where the 12 response coefficients ϕ_i ($i = 1, \dots, 12$) are functions of the 19 invariants

$$\begin{aligned} I_r &= \text{tr } \mathbf{M}_r \mathbf{D}, \quad I_{r+3} = \text{tr } \mathbf{M}_r \mathbf{B} = b_r, \quad I_{r+6} = \text{tr } \mathbf{M}_r \mathbf{D}^2, \\ I_{r+9} &= \text{tr } \mathbf{M}_r \mathbf{B}^2, \quad I_{r+12} = \text{tr } \mathbf{M}_r \mathbf{D} \mathbf{B} \quad (r = 1, 2, 3), \\ I_{16} &= \text{tr } \mathbf{D}^2 \mathbf{B}, \quad I_{17} = \text{tr } \mathbf{D} \mathbf{B}^2, \quad I_{18} = \det \mathbf{D}, \quad I_{19} = \det \mathbf{B}, \end{aligned} \tag{26}$$

subject to the constraints that the deviatoric Cauchy stress has zero trace, and the material is incompressible, so that only 11 coefficients ϕ_i are independent, and only 18 invariants I_j are non-trivial, since $I_{19} = 1$. An alternative constitutive law for the strain rate \mathbf{D} in terms of the deviatoric stress σ' and the strain \mathbf{B} , corresponding to the usual glaciological approach for the isotropic fluid model, can be formulated similarly by interchanging σ' and \mathbf{D} in Equations (25) and (26).

We require that Equation (25) reduces to an isotropic viscous-fluid law

$$\sigma' = \Phi_1 \mathbf{D} + \Phi_2 \left(\mathbf{D}^2 - \frac{1}{3} \text{tr } \mathbf{D}^2 \mathbf{I} \right), \tag{27}$$

where Φ_1, Φ_2 depend on two invariants $\text{tr } \mathbf{D}^2$ and $\det \mathbf{D}$, when there is no fabric; that is, in the initial undeformed state $\mathbf{F} = \mathbf{I}$ when the principal stretches are equal, necessarily $\lambda_1 = \lambda_2 = \lambda_3 = 1$ by the incompressibility condition (Equation (24)), or subsequently when $\mathbf{F} = \mathbf{I}$ or when \mathbf{F} corresponds to a rigid rotation of the ice element. The conventional glaciological model is $\Phi_2 = 0$ and Φ_1 depends only on $\text{tr } \mathbf{D}^2$. The above prescription asserts that there is fabric — some alignment of initially randomly distributed c

axes — only when there are differential principal stretches, i.e. when $\mathbf{B} \neq \mathbf{I}$.

Following Staroszczyk and Morland (in press), we simplify the general law (Equation (25)) by ignoring tensor dependence on \mathbf{D}^2 , \mathbf{B}^2 and \mathbf{DB} , and the terms involving \mathbf{M}_r without \mathbf{D} or \mathbf{B} , i.e. we restrict attention to a reduced model with a linear tensor dependence of σ' on \mathbf{D} and \mathbf{B} . Hence, we adopt the relation

$$\sigma' = \sum_{r=1}^3 \phi_{r+3} \left[\mathbf{M}_r \mathbf{D} + \mathbf{D} \mathbf{M}_r - \frac{2}{3} \text{tr}(\mathbf{M}_r \mathbf{D}) \mathbf{I} \right] + \phi_{12} \left[\mathbf{DB} + \mathbf{BD} - \frac{2}{3} \text{tr}(\mathbf{DB}) \mathbf{I} \right], \tag{28}$$

where the ϕ_{r+3} and ϕ_{12} terms have been modified to recover zero trace, noting that the included scalar $\text{tr}(\mathbf{M}_r \mathbf{D}) = I_r$, and the scalar $\text{tr}(\mathbf{DB}) = I_{13} + I_{14} + I_{15}$. Equation (28) still represents a non-linearly viscous law since, in general, the response functions ϕ_{r+3} and ϕ_{12} depend on \mathbf{D} . We further express these functions in separable forms which factor out invariants depending only on the deformation \mathbf{B} and retain a common dependence on invariants involving the strain rate \mathbf{D} :

$$\phi_{12} = \Phi_0(I_{16}, I_{20}) g(I_{21}, I_{22}), \tag{29}$$

$$\phi_{r+3} = \Phi_0(I_{16}, I_{20}) h(I_{r+3}, I_{21}, I_{22}) \quad (r = 1, 2, 3), \tag{30}$$

where

$$I_{20} = \sum_{r=1}^3 I_{r+6} = \text{tr} \bar{\mathbf{D}}^2, \quad I_{21} = \sum_{r=1}^3 I_{r+3} = \text{tr} \mathbf{B},$$

$$I_{22} = \sum_{r=1}^3 I_{r+9} = \text{tr} \mathbf{B}^2. \tag{31}$$

The response functions (Equations (29) and (30)) have to satisfy the isotropic fluid law (Equation (27)) when $\mathbf{B} = \mathbf{I}$, and hence $I_{21} = I_{22} = 3$; thus

$$\Phi_0(\text{tr} \mathbf{D}^2, \text{tr} \mathbf{D}^2) = \frac{1}{2} \Phi_1(\text{tr} \mathbf{D}^2, \det \mathbf{D}), \quad \Phi_2 = 0, \tag{32}$$

where the functions h and g are normalised by

$$h(1, 3, 3) + g(3, 3) = 1. \tag{33}$$

We restrict attention to a simple model with the fabric response function h depending only on the principal stretches λ_r (through $I_{r+3} = b_r = \lambda_r^2$), and the function g depending only on the invariant measure of total deformation $I_{21} = \text{tr} \mathbf{B}$; thus

$$\Phi_1 = \Phi_1(\text{tr} \mathbf{D}^2) = 2\mu_0, \quad h = h(b_r),$$

$$g = g(K), \quad h(1) + g(3) = 1, \tag{34}$$

where $\mu_0 = 1/\psi_0$ is the (constant) isotropic fluid viscosity (when $b_1 = b_2 = b_3 = 1$), and

$$K = \text{tr} \mathbf{B} = b_1 + b_2 + b_3 \geq 3. \tag{35}$$

Now, with Equations (34) and (32), the constitutive law (Equation (28)) expressed in terms of the two response functions h and g and the viscosity μ_0 takes the linear form

$$\sigma' = \mu_0 \left\{ \sum_{r=1}^3 h(b_r) \left[\mathbf{M}_r \mathbf{D} + \mathbf{D} \mathbf{M}_r - \frac{2}{3} \text{tr}(\mathbf{M}_r \mathbf{D}) \mathbf{I} \right] + g(K) \left[\mathbf{DB} + \mathbf{BD} - \frac{2}{3} \text{tr}(\mathbf{DB}) \mathbf{I} \right] \right\}. \tag{36}$$

Staroszczyk and Morland (in press) derived equalities and inequalities which have to be satisfied by instantaneous

viscosities μ_{ij} ($i, j = 1, 2, 3; i \neq j$), depending on the relative magnitudes of the principal stretches. With the ordering $b_1 \geq b_2 \geq b_3$ there are six distinct sets of relative values of b_r ($r = 1, 2, 3$), and for each of them corresponding relations order μ_{12} , μ_{13} and μ_{23} in the coordinate frame of the principal stretch axes. By using the viscosity relation corresponding to the plane flow, i.e. when $\lambda_2 = b_2 = 1$, hence $b_3 = 1/b_1$ and $K = b_1 + 1 + b_1^{-1}$, it is possible to express $g(K)$ in terms of $h(b_r)$, namely,

$$g(K) = -\frac{b_1}{b_1^2 - 1} [h(b_1) - h(b_1^{-1})], \tag{37}$$

where

$$2b_1 = K - 1 + \sqrt{(K - 1)^2 - 4}, \geq 2. \tag{38}$$

The limit of Equation (37) as $b_1 \rightarrow 1$, $K \rightarrow 3$, combined with the normalisation (34)₄, gives

$$h(1) - h'(1) = 1, \tag{39}$$

which is a restriction on $h(b_r)$ at $b = 1$. Rewriting the function $g(K)$ as

$$g(K) = K^{-1} G(K), \tag{40}$$

where $G(K)$ is bounded, it can be shown that the limit of Equation (37) as $b_1 \rightarrow \infty$, $K \sim b_1$, yields the relation

$$G(\infty) = h(0) - h(\infty). \tag{41}$$

That is, in view of Equation (37), only one fabric response function, $h(b_r)$, remains free for prescription, subject to Equation (39). In order to further restrict this function, the model defined by Equation (36) is used to predict the viscous response of ice at large deformations in the axial compression and simple shear conditions. For such configurations, Budd and Jacka (1989) present experimental data obtained for a steady-state flow (when the microprocesses of grain rotation, polygonisation and dynamic recrystallisation balance one another) and determine the limit ratios of fabric-induced viscosity to (maximum) isotropic viscosity. These empirical ratios, expressed in terms of so-called enhancement factors for compression and shear, provide two further relations connecting $h(\infty)$, $h(0)$ and $G(\infty)$ (Staroszczyk and Morland, in press). For the uniaxial compression the viscous law (Equation (36)) yields

$$\frac{1}{3} h(\infty) + \frac{2}{3} h(0) + \frac{1}{6} G(\infty) = A, \tag{42}$$

where A is the reciprocal of the axial enhancement factor, and for the simple shear in the plane flow we obtain

$$\frac{1}{2} h(\infty) + \frac{1}{2} h(0) + \frac{1}{2} G(\infty) = S, \tag{43}$$

where S is the reciprocal of the shear enhancement factor. Equations (41)–(43) provide the following values of $h(0)$, $h(\infty)$ and $G(\infty)$:

$$h(0) = S, \quad h(\infty) = 6A - 5S, \quad G(\infty) = 6(S - A). \tag{44}$$

Despite several simplifying assumptions adopted to derive the model (36) with the single fabric function $h(b_r)$ from the general orthotropic law (Equation (25)), this approach still retains considerable flexibility to correlate with observed data. In fact, only three specific restrictions are imposed on the function h : Equation (39) to yield a valid response in the isotropic state, and Equations (44)₁ and (44)₂ to match the enhancement factors for compression and sim-

ple shearing at large strains. However, it is also required that the function $h(b_r)$ yield a response which satisfies the viscosity relations derived in Staroszczyk and Morland (in press), otherwise physically invalid responses can be obtained.

4. MODEL COMPARISONS

The two orthotropic models described in sections 2 and 3 are now applied to explore the viscous response of ice to simple deformation histories, corresponding to those taking place in typical laboratory tests. For the sake of brevity, throughout this section we will refer to the micro-macroscopic model as model A, and to the continuum model as model B.

First we consider an axial compression in the x_2 direction, defined by the axial stretch $\lambda_2 < 1$, with equal lateral stretches λ_1 and λ_3 along the x_1 and x_3 coordinate axes, for which the deformation field is described by

$$\begin{aligned} x_1 &= \lambda_1 X_1, \quad x_2 = \lambda_2 X_2, \quad x_3 = \lambda_3 X_3, \\ \lambda_1 &= \lambda_3 > 1, \quad \lambda_2 = \lambda_1^{-2} < 1, \end{aligned} \tag{45}$$

and the associated velocities, in view of Equations (45)₄ and (45)₅ are

$$v_1 = x_1 \dot{\lambda}_1 / \lambda_1, \quad v_2 = -2x_2 \dot{\lambda}_1 / \lambda_1, \quad v_3 = x_3 \dot{\lambda}_1 / \lambda_1. \tag{46}$$

With Equations (45) and (46), the Cauchy–Green strain tensor \mathbf{B} and the strain-rate tensor \mathbf{D} are given by

$$\mathbf{B} = \begin{pmatrix} \lambda_1^2 & 0 & 0 \\ 0 & \lambda_1^{-4} & 0 \\ 0 & 0 & \lambda_1^2 \end{pmatrix}, \quad \mathbf{D} = \begin{pmatrix} \dot{\lambda}_1 / \lambda_1 & 0 & 0 \\ 0 & -2\dot{\lambda}_1 / \lambda_1 & 0 \\ 0 & 0 & \dot{\lambda}_1 / \lambda_1 \end{pmatrix}, \tag{47}$$

and the three structure tensors, due to the coincidence of the principal stretch axes \mathbf{e}_r with the coordinate axes x_r , are defined by

$$\mathbf{M}_1 = \begin{pmatrix} 1 & 0 & 0 \\ 0 & 0 & 0 \\ 0 & 0 & 0 \end{pmatrix}, \quad \mathbf{M}_2 = \begin{pmatrix} 0 & 0 & 0 \\ 0 & 1 & 0 \\ 0 & 0 & 0 \end{pmatrix}, \quad \mathbf{M}_3 = \begin{pmatrix} 0 & 0 & 0 \\ 0 & 0 & 0 \\ 0 & 0 & 1 \end{pmatrix}. \tag{48}$$

The deviatoric stresses (Equations (2)) are given by the diagonal tensor

$$\boldsymbol{\sigma}' = \begin{pmatrix} \sigma'_{11} & 0 & 0 \\ 0 & \sigma'_{22} & 0 \\ 0 & 0 & \sigma'_{33} \end{pmatrix}, \quad \text{with} \quad \sigma'_{11} = \sigma'_{33} = -\sigma'_{22}/2. \tag{49}$$

The response of ice predicted by model A, defined by Equation (14), is illustrated in Figure 2, which shows the evolution of the normalised axial viscosity $\sigma'_{22}/(2\mu_0 D_{22})$ with increasing principal stretch λ_1 for different values of the grain-anisotropy parameter β . The curves corresponding to $\beta = 0.10, 0.15, 0.20, 0.25$ are labelled A1, A2, A3, A4, respectively, and the same labelling applies in subsequent plots illustrating the results given by this model. It is seen from the figure that the micro-macroscopic model predicts very slight softening of ice (decrease in viscosity) during the first stage of uniaxial loading, for the stretches $1 \leq \lambda_1 \lesssim 1.2$ ($0.7 \lesssim \lambda_2 \leq 1$). The softening stage is followed by a phase of considerable hardening of ice, particularly pronounced for the stretches in the range $1.3 \lesssim \lambda_1 \lesssim 1.7$ ($0.35 \lesssim \lambda_2 \lesssim 0.6$) and small values of the parameter β (i.e.

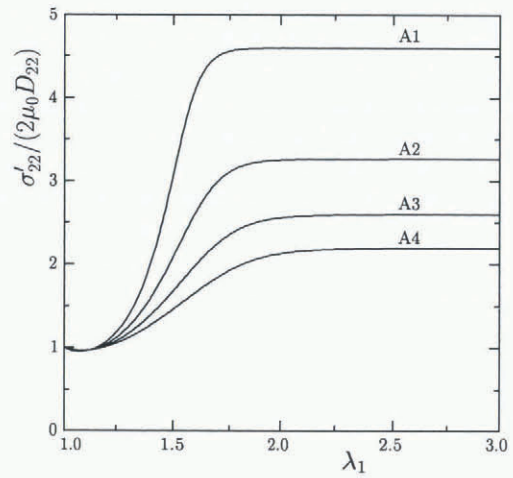


Fig. 2. Evolution of the ratio $\sigma'_{22}/(2\mu_0 D_{22})$ with increasing stretch λ_1 in uniaxial compression for different values of β in model A.

for very anisotropic ice grains). As the deformation continues, all the grain c axes rotate towards the compression axis (here the x_2 axis), and at large strains the macroscopic viscosity of a polycrystal approaches the axial viscosity of a single crystal. Since the latter viscosity is $(1/\beta)$ larger than the viscosity for shearing on crystal basal planes, it follows from Equation (20) that the limit macroscopic viscosity for compression is given in terms of β by the relation

$$\frac{\sigma'_{22}}{2\mu_0 D_{22}} \rightarrow \frac{3\beta + 2}{5\beta}. \tag{50}$$

The viscous response of ice yielded by model B is determined by the function $h(b_r)$. There is a variety of possible functions, as long as they satisfy some very general conditions (Staroszczyk and Morland, in press), and this gives the model ample flexibility to correlate with observations. For illustrations, we apply simple monotonic increasing functions

$$h(b_r) = h_\infty - (h_\infty - h_0) \exp(-\alpha b_r^m), \quad \alpha > 0, \quad n > 0, \quad r = 1, 2, 3 \tag{51}$$

$$h(b_r) = h_0 + (h_\infty - h_0) \tan(\alpha b_r), \quad \alpha > 0, \tag{52}$$

where $h_0 = h(0)$ and $h_\infty = h(\infty)$, m in Equation (51) is a free parameter, and α in Equations (51) and (52) is determined by Equation (39). The limit values $h(0)$ and $h(\infty)$ are related through Equations (44) to A and S , the reciprocals of the enhancement factors. In Staroszczyk and Morland (in press) both A and S were chosen less than unity (both enhancement factors greater than unity), which corresponds to the values measured by Budd and Jacka (1989) for warm ice near melting. Here, in order to compare the predictions of the two orthotropic models, we adopt $A > 1$ (an enhancement factor for compression less than unity), meaning the increase in viscosity with increasing deformation, which according to Pimienta and others (1987) is the case for the response of cold ice subjected to stress levels typically occurring in polar ice sheets. The value of A can be as high as 10 for a single-maximum fabric, as has been found experimentally by Pimienta and others (1987), although recently Mangeney and others (1996) calculated the value of about 3 for the ice near the bottom of the GRIP ice core, deduced from the data provided by Thorsteinsson and others (1997). We carry out the simulations for two values of this factor, namely, $A = 2.2$, which is smaller, and $A = 4.6$, which is larger than the value obtained for the GRIP ice, though both orthotropic models are flexible

in this respect and allow much larger values of A to be implemented. Since Expression (50), defining the asymptotic value of viscosity, is simply the reciprocal of the enhancement factor, A , it relates the parameter A in model B to the parameter β in model A. Hence, we find that the selected values $A = 2.2$ and $A = 4.6$ correspond to $\beta = 0.25$ and $\beta = 0.10$, respectively. Associated with the chosen values of A are the factors $S = 0.55$ and $S = 0.46$, being the limit values of the normalised viscosity in simple shear, which correspond, respectively, to $\beta = 0.25$ and $\beta = 0.10$ in model A, as will be shown shortly in Figure 6. In view of Equations (44), we have the following connections:

$$\beta = 0.10: A = 4.60, S = h(0) = 0.46, h(\infty) = 25.30, \tag{53}$$

$$\beta = 0.25: A = 2.20, S = h(0) = 0.55, h(\infty) = 10.45. \tag{54}$$

The response functions h determined by the limit values in Equations (54) are illustrated in Figure 3, and very similar plots can be obtained for Equations (53). Henceforth, the curves labelled B1, B2, B3 correspond to Equation (51) with $m = 1, 1.5, 2$, respectively, and the curves labelled B4 correspond to Equation (52).

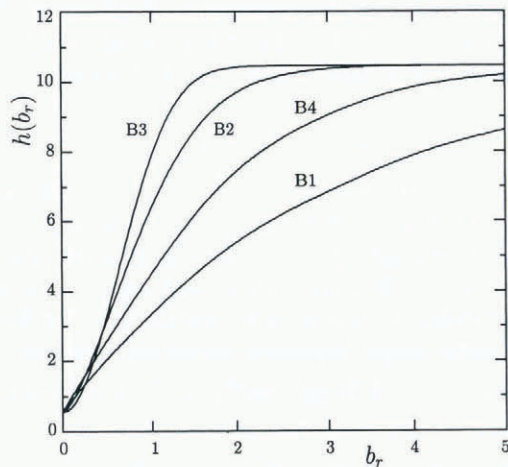


Fig. 3. Adopted forms of the fabric response function $h(b_r)$ in model B.

With Equations (47–49), the constitutive law (Equation (36)) leads to the following relation describing the behaviour of ice in uniaxial compression:

$$\frac{\sigma'_{22}}{2\mu_0 D_{22}} = \frac{1}{3} [h(b_1) + 2h(b_1^{-2}) + g(K)(b_1 + 2b_1^{-2})], \tag{55}$$

where $K = 2b_1 + b_1^{-2}$. The evolution of the axial viscosity $\sigma'_{22}/(2\mu_0 D_{22})$ with increasing stretch λ_1 for the adopted forms of the fabric response function $h(b_r)$ is illustrated in Figure 4 for the parameters in Equation (53), and in Figure 5 for the parameters in Equations (54). We note that the influence of the function $h(b_r)$ on the predicted response of ice is most significant during the first phase of deformation. We see that the functions in Equation (51) with $m = 1.5$ and $m = 2$, curves B2 and B3, respectively, yield responses which agree quite well with the responses given by model A, curves A1 and A4, particularly for the set of parameters in Equations (54).

Next we consider a simple shear at constant strain rate $D_{12} = \frac{1}{2} \dot{\gamma}$ which follows an initial plane compression and

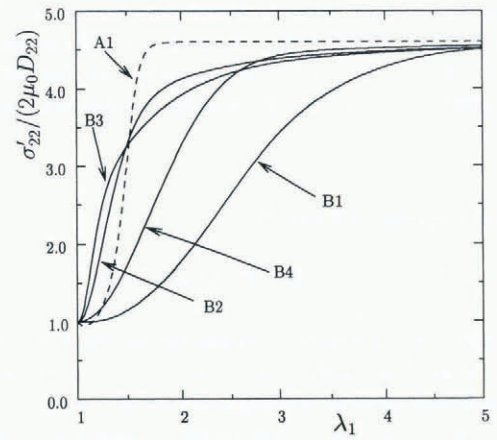


Fig. 4. Evolution of the ratio $\sigma'_{22}/(2\mu_0 D_{22})$ with increasing stretch λ_1 in uniaxial compression for different fabric response functions $h(b_r)$ in model B. The results for $A = 4.6$ and $S = 0.46$ are compared with the prediction of model A for $\beta = 0.10$.

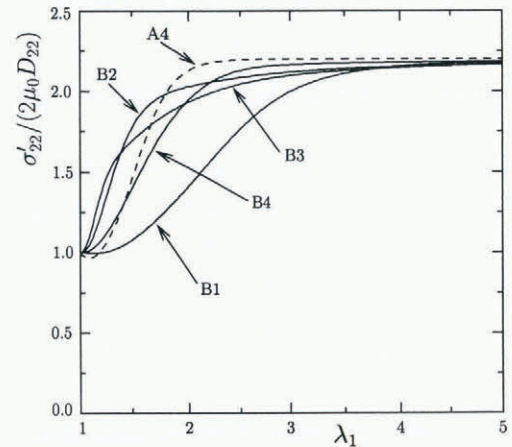


Fig. 5. Evolution of the ratio $\sigma'_{22}/(2\mu_0 D_{22})$ with increasing stretch λ_1 in uniaxial compression for different fabric response functions $h(b_r)$ in model B. The results for $A = 2.2$ and $S = 0.55$ are compared with the prediction of model A for $\beta = 0.25$.

stretch that has been frozen at constant $\lambda_2 = \lambda_1^{-1} \leq 1$ by the removal of the stress and strain rate. The deformation field is now described by

$$x_1 = \lambda_1 X_1 + \kappa X_2, \quad x_2 = \lambda_1^{-1} X_2, \quad x_3 = X_3, \tag{56}$$

the corresponding velocities are

$$v_1 = x_2 \dot{\kappa} \lambda_1, \quad v_2 = v_3 = 0, \quad \dot{\kappa} = \dot{\gamma} \lambda_1^{-1}, \tag{57}$$

and the strain and strain-rate tensors are defined by

$$\mathbf{B} = \begin{pmatrix} \lambda_1^2 + \kappa^2 & \lambda_1^{-1} \kappa & 0 \\ \lambda_1^{-1} \kappa & \lambda_1^{-2} & 0 \\ 0 & 0 & 1 \end{pmatrix}, \quad \mathbf{D} = \begin{pmatrix} 0 & \frac{1}{2} \dot{\gamma} & 0 \\ \frac{1}{2} \dot{\gamma} & 0 & 0 \\ 0 & 0 & 0 \end{pmatrix}. \tag{58}$$

The principal stretch squares b_i ($i = 1, 2, 3$), the eigenvalues of \mathbf{B} , are given by

$$2b_1 = \lambda_1^2 + \lambda_1^{-2} + \kappa^2 + \sqrt{(\lambda_1^2 + \lambda_1^{-2} + \kappa^2)^2 - 4}, \tag{59}$$

$$b_2 = b_1^{-1}, \quad b_3 = 1,$$

and the associated principal vectors \mathbf{e}_r are determined by

Equation (22)₂. In terms of these vectors, the three structure tensors are expressed by

$$M_s = \begin{pmatrix} e_s^{(1)} e_s^{(1)} & e_s^{(1)} e_s^{(2)} & 0 \\ e_s^{(1)} e_s^{(2)} & e_s^{(2)} e_s^{(2)} & 0 \\ 0 & 0 & 0 \end{pmatrix} (s = 1, 2), \quad M_3 = \begin{pmatrix} 0 & 0 & 0 \\ 0 & 0 & 0 \\ 0 & 0 & 1 \end{pmatrix}. \tag{60}$$

The response of ice to simple shearing given by model A, defined by Equation (14), is illustrated in Figure 6, which shows the evolution of the normalised viscosity $\sigma'_{12}/(\mu_0\dot{\gamma})$ with increasing shear κ started from the isotropic state ($\lambda_1 = \lambda_2 = 1$) for different values of the grain-anisotropy parameter β . We note that the model predicts initial hardening of ice (for strains $\kappa \lesssim 1$), with a more significant increase in viscosity taking place for smaller values of β (i.e. for more anisotropic ice grains). As shearing continues, the initial hardening is followed by the softening phase, with a monotonic decrease in viscosity until an asymptotic value is reached at large strains. This limit value is given by

$$\frac{\sigma'_{12}}{\mu_0\dot{\gamma}} \rightarrow \frac{3\beta + 2}{5}, \tag{61}$$

and follows from Equation (20), since at very large shear deformations all crystals are aligned for easy glide on basal planes (their c axes are approximately parallel to one another) and hence in the limit the macroscopic viscosity of a polycrystal approaches the viscosity of an individual grain.

In Figure 6 we also show the results predicted by a discrete grain model, with 800 grains, for $\beta = 0.10$ (curve D1), and $\beta = 0.25$ (curve D4). The discrete model is based on the same assumptions as model A, except that no restrictions on material symmetries are imposed, so it has a more general character than the orthotropic model. Therefore, comparisons between the predictions of both models should give some indication whether the assumption of orthotropy of ice is justified. The results obtained seem to support the validity of this assumption, since the maximum relative discrepancies between curves A1 and D1, and A4 and D4, do not exceed 15% for $\kappa \sim 1$, and for larger shear strains ($\kappa \gtrsim 5$) the agreement between the results given by both models is very good.

The behaviour of ice predicted by model B, defined by

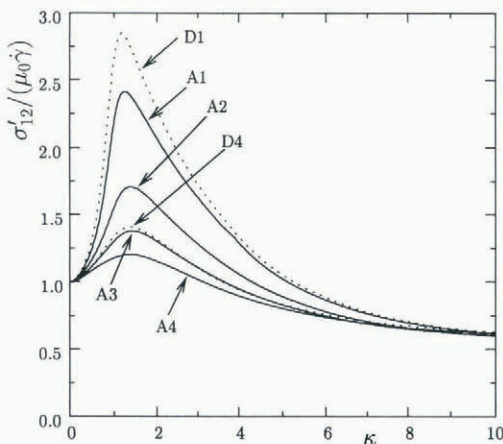


Fig. 6. Evolution of the ratio $\sigma'_{12}/(\mu_0\dot{\gamma})$ with increasing strain κ in simple shear started from an isotropic state ($\lambda_2 = 1$) for different values of β in model A. Also shown are the results given by the discrete grain model for $\beta = 0.10$ (curve D1) and $\beta = 0.25$ (curve D4).

Equation (36) with Equations (58–60), is described by

$$\frac{\sigma'_{12}}{\mu_0\dot{\gamma}} = \frac{1}{2} [h(b_1) + h(b_1^{-1}) + g(K)(\lambda_1^2 + \lambda_1^{-2} + \kappa^2)], \tag{62}$$

where now $K = b_1 + b_1^{-1} + 1$. Figures 7 and 8 show, for different fabric response functions (Equations (51) and (52)), the evolution of the viscosity ratio $\sigma'_{12}/(\mu_0\dot{\gamma})$ with shear κ started from the isotropic state ($\lambda_1 = \lambda_2 = 1$). The same sets of parameters as in the uniaxial compression simulations are used, i.e. those in Equation (53) for Figure 7 and those in Equation (54) for Figure 8, and again the results yielded by model B are compared with the predictions of the micro-macroscopic model A (curves A1 and A4). It can be observed that now, for simple shear, the discrepancies between the responses given by the two models are more considerable than in the case of uniaxial compression, especially for the parameters in Equation (53) (Fig. 7), corresponding to more anisotropic grains (smaller value of β) in model A, or “stiffer” ice (larger value of the viscosity factor A) in model B. For the parameters in Equation (54) (Fig. 8), a good qualitative agreement between the two models is still reached, although model A predicts more significant increase in ice viscosity

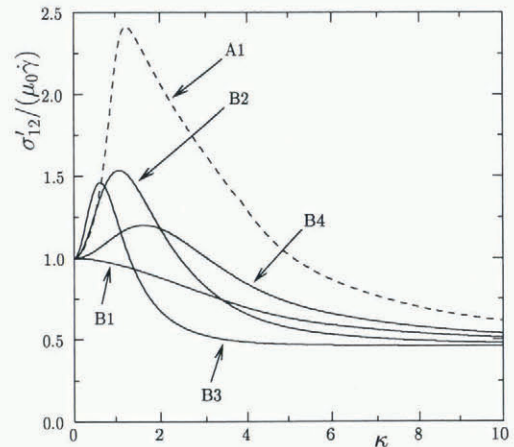


Fig. 7. Evolution of the ratio $\sigma'_{12}/(\mu_0\dot{\gamma})$ with increasing strain κ in simple shear started from an isotropic state ($\lambda_2 = 1$) for different fabric response functions $h(b_r)$ in model B. The results for $A = 4.6$ and $S = 0.46$ are compared with the prediction of model A for $\beta = 0.10$.

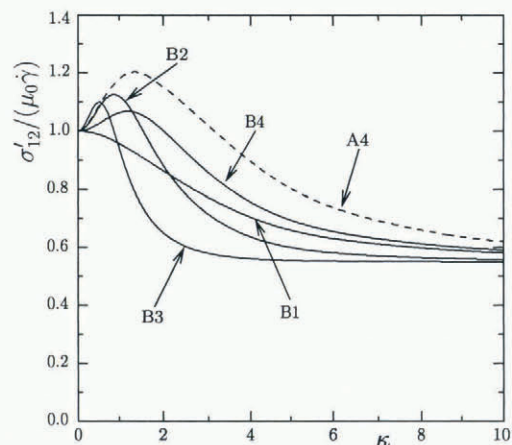


Fig. 8. Evolution of the ratio $\sigma'_{12}/(\mu_0\dot{\gamma})$ with increasing strain κ in simple shear started from an isotropic state ($\lambda_2 = 1$) for different fabric response functions $h(b_r)$ in model B. The results for $A = 2.2$ and $S = 0.55$ are compared with the prediction of model A for $\beta = 0.25$.

during the initial phase of shearing. However, the discrepancies between the two models are still limited to relatively small (compared to those occurring in ice-sheet flows) shear strains, so it is anticipated that in realistic ice-sheet flow simulations the two constitutive theories should yield similar predictions for most of an ice sheet, apart from a region near the ice divide, where (relatively) small shear deformations occur.

5. CONCLUSIONS

We have presented two orthotropic models for viscous response of ice based on two fundamentally different approaches. The first, a micro-macroscopic model, has been derived from the behaviour of individual ice grains and incorporates the mechanism of crystal rotation in response to shear stresses. The second, a macroscopic model, was constructed by applying the general theory of frame-indifferent (objective) relations for materials with orthotropic anisotropy. The results of numerical simulations for continued uniaxial compression and simple shearing have shown that for appropriately chosen model parameters a good correlation between the responses given by the two theories can be achieved. Both models predict significant hardening of ice in compression, and initial hardening followed by softening in simple shear, which seems to agree with the observed behaviour of cold ice at low stress levels. The theoretical results, however, should be verified against detailed experimental data; unfortunately, very few relevant data on cold ice are available, since practically all laboratory tests performed to date have been carried out on warm ice near melting and at relatively high deviatoric stresses. It is also anticipated that the numerical simulations of realistic ice-sheet flows and the comparison of results obtained in this way with in situ data should throw some light on the validity of the assumptions made in the paper: first of all, whether the assumption of orthotropic behaviour of ice is justified, or a more general form of anisotropic constitutive law is required.

Further work should concentrate on including in the models other micromechanisms, such as rotation and migration (dynamic) recrystallisation. This will, however, add considerably to the complexity of theoretical formulations. This is particularly true of the micro-macroscopic model, and, to the authors' knowledge, very few attempts to incorporate recrystallisation have yet been made. In terms of extending its generality, the continuum model is more flexible, since only the modification of response functions is required, although in order to account for a more complex mechanical behaviour more tensor generators may be needed in the constitutive law. Finally, we would like to emphasise that in order to construct a model that properly describes the behaviour of ice in polar ice sheets, more experimental work on cold ice needs to be done to provide reliable input data for the theory.

ACKNOWLEDGEMENTS

The authors would like to thank two anonymous referees for thorough reviews that have helped to improve the paper. Part of this work was done while the first author was visiting the Laboratoire de Glaciologie, Saint-Martin-d'Hères, France, supported by EISMINT Exchange Grant No. 9709 funded by the European Science Foundation.

REFERENCES

- Alley, R. B. 1992. Flow-law hypotheses for ice-sheet modeling. *J. Glaciol.*, **38**(129), 245–256.
- Azuma, N. 1994. A flow law for anisotropic ice and its application to ice sheets. *Earth Planet. Sci. Lett.*, **128**(3–4), 601–614.
- Azuma, N. and K. Goto-Azuma. 1996. An anisotropic flow law for ice-sheet ice and its implications. *Ann. Glaciol.*, **23**, 202–208.
- Boehler, J. P. 1987. Representations for isotropic and anisotropic non-polynomial tensor functions. In Boehler, J. P., ed. *Application of tensor functions in solid mechanics*. Berlin, etc., Springer-Verlag. International Centre for the Mechanical Sciences, 31–53. (Course 292.)
- Budd, W. F. and T. H. Jacka. 1989. A review of ice rheology for ice sheet modelling. *Cold Reg. Sci. Technol.*, **16**(2), 107–144.
- Bunge, H. J. 1982. *Texture analysis in material science*. London, Butterworths.
- Castelnau, O. and P. Duval. 1994. Simulations of anisotropy and fabric development in polar ices. *Ann. Glaciol.*, **20**, 277–282.
- Castelnau, O., P. Duval, R. Lebensohn and G. R. Canova. 1996. Viscoplastic modeling of texture development in polycrystalline ice with a self-consistent approach: comparison with bound estimates. *J. Geophys. Res.*, **101**(B6), 13,851–13,868.
- Gagliardini, O. and J. Meyssonier. In press. Analytical derivations for the behaviour and fabric evolution of a linear orthotropic ice polycrystal. *J. Geophys. Res.*
- Gödert, G. and K. Hutter. 1998. Induced anisotropy in large ice shields: theory and its homogenization. *Continuum Mech. Thermodyn.*, **10**(5), 293–318.
- Gödert, G. and K. Hutter. In press. A kinematic model for induced anisotropy in large ice shields. *Proc. R. Soc. London*.
- Gow, A. J. and T. Williamson. 1976. Rheological implications of the internal structure and crystal fabrics of the West Antarctic ice sheet as revealed by deep core drilling at Byrd Station. *Geol. Soc. Am. Bull.*, **87**(12), 1665–1677.
- Herron, S. L. and C. C. Langway, Jr. 1982. A comparison of ice fabrics and textures at Camp Century, Greenland and Byrd Station, Antarctica. *Ann. Glaciol.*, **3**, 118–124.
- Johnson, A. F. 1977. Creep characterization of transversely-isotropic metallic material. *J. Mech. Phys. Solids*, **25**, 117–126.
- Lipenkov, V. Ya., N. I. Barkov, P. Duval and P. Pimienta. 1989. Crystalline texture of the 2083 m ice core at Vostok Station, Antarctica. *J. Glaciol.*, **35**(121), 392–398.
- Lliboutry, L. 1993. Anisotropic, transversely isotropic nonlinear viscosity of rock ice and rheological parameters inferred from homogenization. *Int. J. Plasticity*, **9**(5), 619–632.
- Lliboutry, L. and P. Duval. 1985. Various isotropic and anisotropic ices found in glaciers and polar ice caps and their corresponding rheologies. *Ann. Geophys.*, **3**(2), 207–224.
- Mangency, A., F. Califano and O. Castelnau. 1996. Isothermal flow of an anisotropic ice sheet in the vicinity of an ice divide. *J. Geophys. Res.*, **101**(B12), 28,189–28,204.
- Mangency, A., F. Califano and K. Hutter. 1997. A numerical study of anisotropic, low Reynolds number, free surface flow for ice sheet modeling. *J. Geophys. Res.*, **102**(B10), 22,749–22,764.
- Meyssonier, J. and A. Philip. 1996. A model for the tangent viscous behaviour of anisotropic polar ice. *Ann. Glaciol.*, **23**, 253–261.
- Morland, L. and R. Staroszczyk. 1998. Viscous response of polar ice with evolving fabric. *Continuum Mech. Thermodyn.*, **10**(3), 135–152.
- Pimienta, P., P. Duval and V. Ya. Lipenkov. 1987. Mechanical behavior of anisotropic polar ice. *International Association of Hydrological Sciences Publication 170* (Symposium at Vancouver 1987 — *The Physical Basis of Ice Sheet Modelling*), 57–66.
- Russell-Head, D. S. and W. F. Budd. 1979. Ice-sheet flow properties derived from bore-hole shear measurements combined with ice-core studies. *J. Glaciol.*, **24**(90), 117–130.
- Staroszczyk, R. and L. Morland. In press. Orthotropic viscous response of polar ice. *J. Eng. Math.*
- Svensden, B. and K. Hutter. 1996. A continuum approach for modelling induced anisotropy in glaciers and ice sheets. *Ann. Glaciol.*, **23**, 262–269.
- Taylor, G. I. 1938. Plastic strain in metals. *J. Inst. Met.*, **62**, 307–324.
- Thorsteinsson, Th., J. Kipfstuhl and H. Miller. 1997. Textures and fabrics in the GRIP ice core. *J. Geophys. Res.*, **102**(C12), 26,583–26,600.
- Van der Veen, C. J. and I. M. Whillans. 1990. Flow laws for glacier ice: comparison of numerical predictions and field measurements. *J. Glaciol.*, **36**(124), 324–339.
- Van der Veen, C. J. and I. M. Whillans. 1994. Development of fabric in ice. *Cold Reg. Sci. Technol.*, **22**(2), 171–195.